Discover Oncology

Research

Preoperative discrimination of invasive and non-invasive breast cancer using machine learning based on automated breast volume scanning (ABVS) radiomics and virtual touch quantification (VTQ)

Lifang Fan[1,2] · Yimin Wu[3] · Shujian Wu[4] · Chaoxue Zhang[1] · Xiangming Zhu[4]

Received: 25 December 2023 / Accepted: 8 October 2024
Published online: 16 October 2024

Abstract

Purpose Evaluating the efficacy of machine learning for preoperative differentiation between invasive and non-invasive breast cancer through integrated automated breast volume scanning (ABVS) radiomics and virtual touch quantification (VTQ) techniques.

Methods We conducted an extensive retrospective analysis on a cohort of 171 breast cancer patients, differentiating them into 124 invasive and 47 non-invasive cases. The data was meticulously divided into a training set (n = 119) and a validation set (n = 52), maintaining a 70:30 ratio. Several machine learning models were developed and tested, including Logistic Regression (LR), Random Forest (RF), Decision Tree (DT), and Support Vector Machine (SVM). Their performance was evaluated using the Area Under the Receiver Operating Characteristic (ROC) Curve (AUC), and visualized the feature contributions of the optimal model using Shapley Additive Explanations (SHAP).

Results Through both univariate and multivariate logistic regression analyses, we identified key independent predictors in differentiating between invasive and non-invasive breast cancer types: coronal plane features, Shear Wave Velocity (SWV), and Radscore. The AUC scores for our machine learning models varied, ranging from 0.625 to 0.880, with the DT model demonstrating a notably high AUC of 0.874 in the validation set.

Conclusion Our findings indicate that machine learning models, which integrate ABVS radiomics and VTQ, are significantly effective in preoperatively distinguishing between invasive and non-invasive breast cancer. Particularly, the DT model stood out in the validation set, establishing it as the primary model in our study. This highlights its potential utility in enhancing clinical decision-making processes.

Keywords Machine learning · Automated breast volume scanning · Radiomics · Virtual touch quantification · Breast cancer

Lifang Fan and Yimin Wu have made an equal contribution to this article and share first authorship.

✉ Chaoxue Zhang, zcxay@163.com; ✉ Xiangming Zhu, zhuxmwuhu@163.com | [1]The First Affiliated Hospital of Anhui Medical University, No. 218, Jixi Road, Shushan District, Hefei, Anhui Province, China. [2]School of Medical Imageology, Wannan Medical College, Wuhu, Anhui, China. [3]Department of Ultrasound, WuHu Hospital, East China Normal University (The Second People's Hospital, WuHu), Wuhu, Anhui, China. [4]Yijishan Hospital of Wannan Medical College, No. 2 Zheshan West Road, Jinghu District, Wuhu 241001, Anhui Province, China.

1 Introduction

Breast cancer remains the predominant malignant neoplasm in women, characterized by its high prevalence and mortality rates [1, 2]. Despite this, the development of effective preventive strategies for breast cancer is still in its nascent stages [3]. Accurately distinguishing between invasive and non-invasive breast cancer preoperatively is essential in guiding surgical approach selection and prognostic evaluation for patients [4]. Presently, this differentiation largely depends on histopathological examination results. However, advancements in medical imaging technologies are increasingly contributing valuable insights [5]. Radiomics, leveraging high-throughput methodologies, extracts a multitude of quantitative features from medical images—features often imperceptible to the human eye. When these radiomic features are synthesized with imaging findings and clinical data, they significantly refine the precision of preoperative diagnoses, thereby informing treatment decisions and potentially enhancing patient outcomes [6–8].

Automated Breast Volume Scanning (ABVS) represents a novel, non-radiating, and non-invasive approach, offering a painless and safe alternative for comprehensive breast examination. It utilizes a specialized high-frequency broadband transducer to automatically scan the breast, producing standardized, repeatable, and high-resolution images that encompass extensive breast data [9]. Concurrently, Virtual Touch Tissue Quantification (VTQ), a modality of Acoustic Radiation Force Impulse (ARFI) elastography, quantifies tissue stiffness through Shear Wave Velocity (SWV) measurements. This technique correlates tissue hardness with SWV values, where harder tissues exhibit higher SWV [10–12]. Our study investigates the integration of ABVS radiomics with VTQ in conjunction with machine learning methodologies to enhance the preoperative differentiation between invasive and non-invasive breast cancer, aiming to contribute a novel perspective in breast cancer diagnostics.

2 Materials and methods

2.1 Study population

A retrospective analysis was performed on the complete records of 258 breast cancer patients diagnosed via surgical pathology and immunohistochemistry at Wuhu City's Second People's Hospital between October 2020 and May 2023. Inclusion criteria included: (1) availability of complete ultrasonographic and clinical pathological data; (2) no prior exposure to neoadjuvant radiotherapy, chemotherapy, or other non-surgical treatments before surgery. Exclusion criteria were applied to cases with unclear lesion presentation. After applying these inclusion and exclusion criteria, a total of 171 patients met the study requirements. This cohort comprised 124 invasive breast cancer patients aged 30 to 83 years, with a mean age of 55.0 ± 11.1 years, and 47 non-invasive breast cancer patients aged 35 to 85 years, with a mean age of 56.5 ± 11.6 years. Patients were randomly divided into a training set (119 patients) and a validation set (52 patients) in a 7:3 ratio, as outlined in the patient selection flowchart (Fig. 1). The study was ethically reviewed and approved by the Ethics Committee of Wannan Medical College (IRB No. 102, 2023). As this study is a retrospective analysis, the requirement for informed consent was waived by the Ethics Committee.

2.2 Instruments and methods

Conventional ultrasound examinations were meticulously conducted using the Siemens Acuson S2000 diagnostic system. This system was outfitted with a 14L5 high-frequency probe, operating within a frequency range of 7–14 MHz and equipped with ARFI imaging software. The imaging and assessments were performed by two seasoned sonographers, each boasting over a decade of experience in the field. Following the standard ultrasound protocol, the probe was switched to VTQ mode to examine the lesion's largest longitudinal or transverse section. We carefully adjusted the Regions of Interest (ROIs) to an optimal size, and patients were instructed to hold their breath for a brief period of 3–5 s. Within the targeted plane, the ROIs was strategically marked, deliberately avoiding areas of calcification, cystic changes, or necrotic tissue. Subsequently, acoustic pulses were deployed to measure the SWV, thereby assessing the tissue's elastic properties within the ROIs, with the results presented in meters per second.

For the ABVS examination, a 14L5BV free-arm volume probe, featuring a frequency range of 5–14 MHz, was employed. Patients underwent scanning in either a supine or lateral position to ensure comprehensive coverage in the

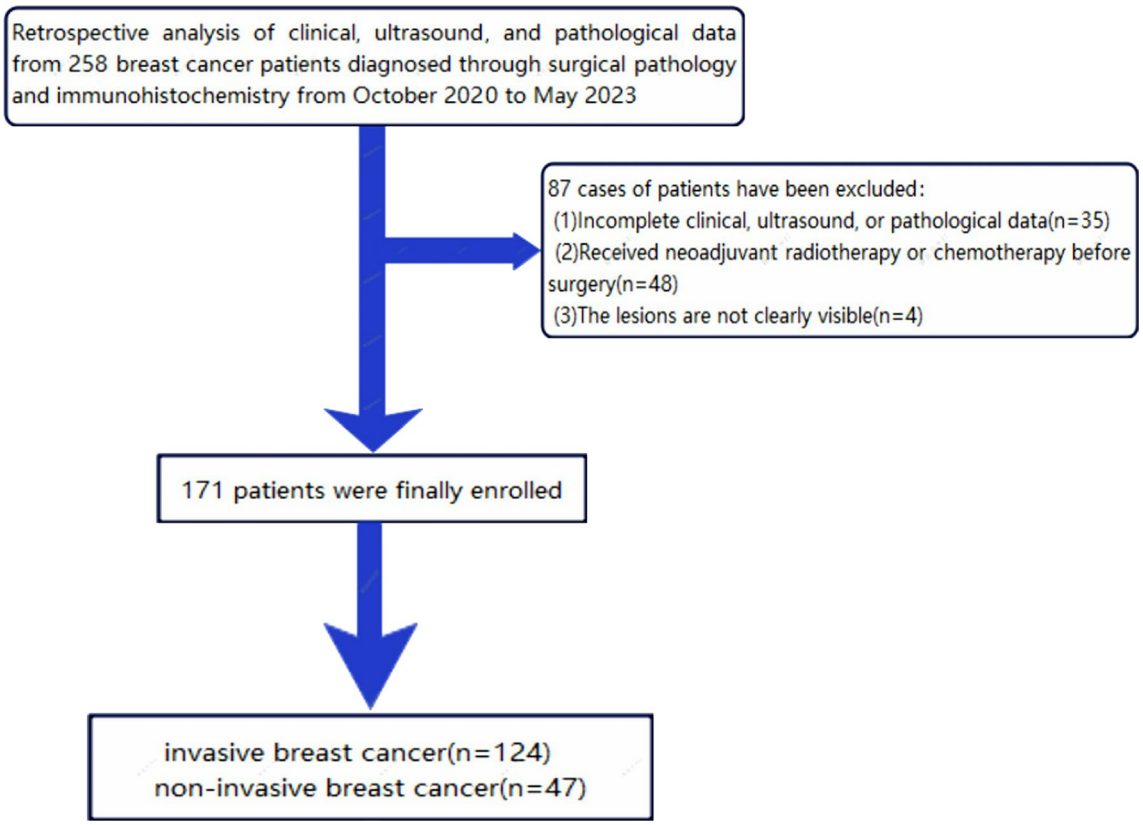

Fig. 1 The flow chart for patient selection

anterior–posterior, lateral, and medial orientations. For patients with larger breasts, additional scans of the superior-inferior segments were conducted. Post-examination, the data were transferred to the ABVS post-processing workstation for the generation of fundamental planar images and the execution of three-dimensional reconstruction of the coronal plane. The analysis of ABVS images concentrated on delineating the characteristics of the breast lesion, including echo patterns, shape, margins, aspect ratio, spiculated halo, microcalcifications, retraction sign, posterior echoes, blood flow signals, ductal dilatation, and features specific to the coronal plane. In instances of diagnostic discrepancy, the two physicians engaged in thorough discussion until a consensus was reached, ensuring the utmost accuracy in our findings.

2.3 Tumor segmentation

The coronal three-dimensional images obtained from the ABVS were meticulously exported from the workstation. To ensure uniformity, all images initially underwent standardization utilizing the advanced MaZda software. Following this, the two experienced ultrasound physician independently outlined the ROIs around each identified lesion. In delineating the ROIs, utmost care was exercised to encase the entire lesion while precisely maintaining within its boundaries to ensure accuracy. To evaluate the consistency of the features extracted by both physicians, we employed the Intraclass Correlation Coefficient (ICC). Only those features demonstrating high consistency (ICC > 0.8) were retained for further analysis. This rigorous approach resulted in the extraction of a comprehensive set of 298 radiomics features, encompassing a diverse array of characteristics such as gray-level histograms, gray-level co-occurrence matrices, run-length matrices, absolute gradients, autoregressive models, and wavelet transforms. To refine our dataset and isolate the most impactful features, we applied the sophisticated Least Absolute Shrinkage and Selection Operator (LASSO) logistics regression algorithm, a method renowned for its effectiveness in dimensionality reduction. The culmination of this process was the calculation of the radiomics score (Radscore), which was determined based on the weighted significance of each selected feature. This methodical and detailed approach underscores our commitment to precision and reliability in radiomics analysis. The workflow of the radiomics analysis is depicted in Fig. 2.

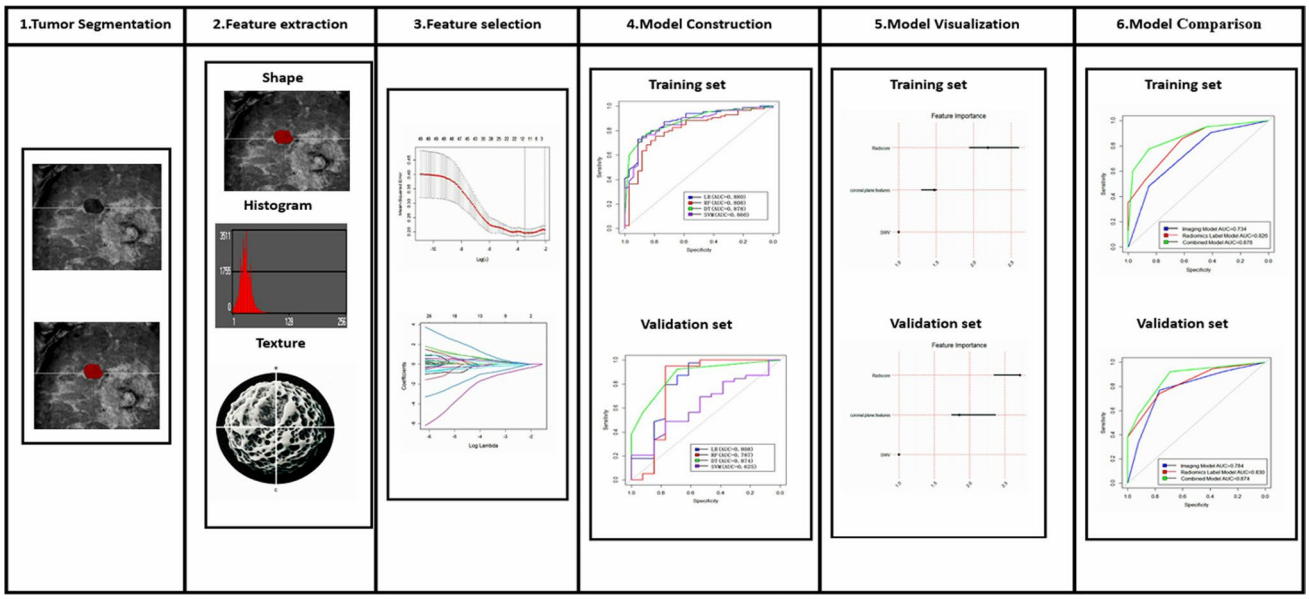

Fig. 2 Workflow for the radiomics process

2.4 Statistical methods

Categorical variables in our study were meticulously analyzed using either the Chi-square test or Fisher's exact probability test, depending on their appropriateness. For continuous variables, we employed the t-test to ensure rigorous statistical examination. To identify independent factors influencing our study outcomes, both univariate and multivariate logistic regression analyses were conducted. In terms of model construction, we utilized four sophisticated machine learning algorithms: Logistic Regression (LR), Random Forest (RF), Decision Tree (DT), and Support Vector Machine (SVM). The diagnostic performance of these models was comprehensively evaluated based on several key metrics: the Area Under the Receiver Operating Characteristic (ROC) Curve (AUC), along with sensitivity and specificity. Throughout our study, a *P*-value less than 0.05 was stringently adhered to as the criterion for statistical significance.

3 Results

3.1 General information

Within both the training and validation sets, statistically significant differences were observed in the coronal plane characteristics and SWV between invasive and non-invasive breast cancer groups ($P < 0.05$). No significant differences were found in other aspects ($P > 0.05$) (Table 1)."

3.2 Radiomics score labeling

Initially, the extracted radiomics features underwent Z-score standardization. Subsequent dimensionality reduction using LASSO logistics regression identified 12 optimal radiomics features (Fig. 3). Based on these features, a Radscore was established. In the training set, the Radscores for invasive cancer were 0.76 ± 0.13 and for non-invasive cancer were 0.60 ± 0.13. The difference between these two groups was statistically significant ($t = 6.188$, $P < 0.001$). In the validation set, the Radscores for invasive cancer were 0.72 ± 0.13 and for non-invasive cancer were 0.57 ± 0.14. The difference between these groups was also statistically significant ($t = 3.321$, $P = 0.002$) (Fig. 4).

Table 1 Comparative analysis of general data between the training set and validation set for invasive and non-invasive breast cancer

Characteristic		Training set (n = 119)		t/x^2	*P*	Validation set (n = 52)		t/x^2	*P*
		Invasive breast cancer (n = 85)	Non-invasive breast cancer (n = 34)	Value	Value	Invasive breast cancer (n = 39)	Non-invasive breast cancer (n = 13)	Value	Value
Age		55.6 ± 11.8	55.9 ± 10.1	−0.117*	0.907	53.8 ± 9.5	58.2 ± 15.4	−1.207*	0.233
Echogenicity mode				0.030	0.862				
	Low echogenicity	80	31			38	11	2.891	0.089
	Mixed echogenicity	5	3			1	2		
Shape				0.026	0.873			0.680	0.410
	Regular	3	1			1	1		
	Irregular	82	33			38	12		
Margin				0.336	0.562			0.453	0.501
	Clear	20	10			12	6		
	Unclear	65	24			27	7		
Aspect ratio				2.169	0.141			1.675	0.196
	< 1	53	26			12	1		
	≧1	32	8			27	12		
Ductal branching				1.220	0.269			2.085	0.149
	Present	59	20			31	7		
	Absent	26	14			8	6		
Microcalcifications				2.720	0.099			1.733	0.188
	Present	54	16			13	7		
	Absent	31	18			26	6		
Retraction sign				1.488	0.223			0.231	0.631
	Present	48	15			21	6		
	Absent	37	19			18	7		
Posterior acoustic features				0.573	0.449			0.028	0.868
	Weakened	24	12			15	4		
	Unchanged/enhanced	61	22			24	9		
Blood flow signal				0.247	0.619			0.055	0.815
	0-I	13	4			6	1		
	II-III	72	30			33	12		
Ductal dilation				1.288	0.256			2.085	0.149
	Present	19	11			8	6		
	Absent	66	23			31	7		
Coronal plane features				10.826	0.004			7.499	0.024
	No specific signs	27	17			14	7		

Table 1 (continued)

Characteristic		Training set (n = 119)		t/x^2	*P*	Validation set (n = 52)		t/x^2	*P*
		Invasive breast cancer (n = 85)	Non-invasive breast cancer (n = 34)	Value	Value	Invasive breast cancer (n = 39)	Non-invasive breast cancer (n = 13)	Value	Value
	Perforation sign	18	12			6	5		
	Convergence sign	40	5			19	1		
SWV (m/s)				10.905	0.001			5.200	0.023
	< 9	15	16			6	6		
	≧9	70	18			33	7		

* represents the t-value, while the rest are chi-square (x^2) values

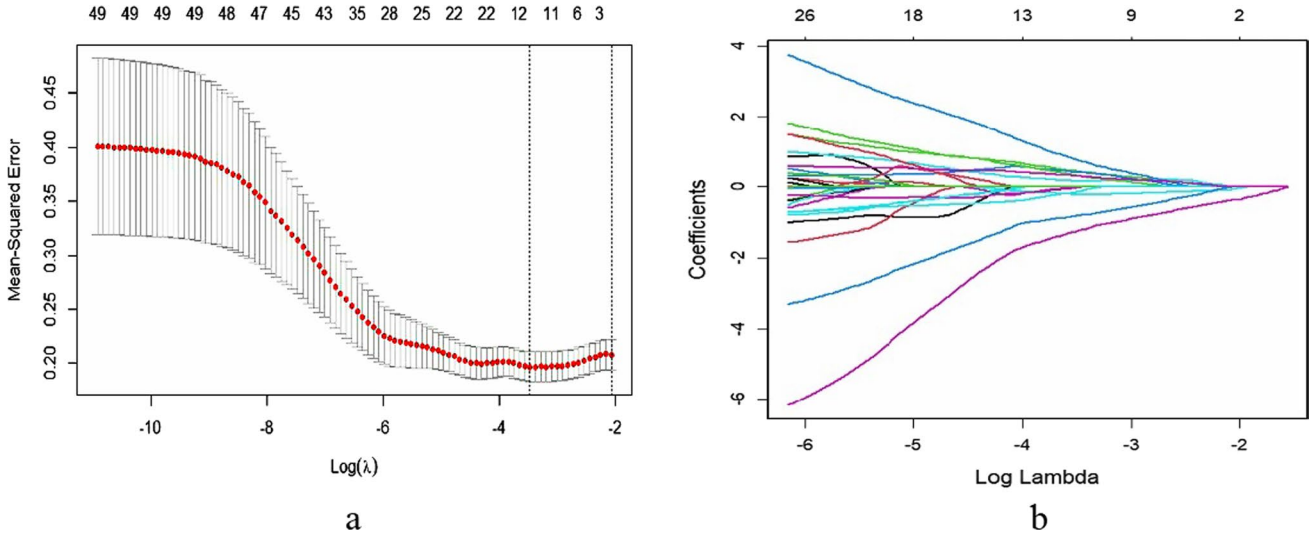

Fig. 3 Lasso regression curves. **a** The regression analysis was conducted with tenfold cross-validation to select the optimal radiomic features for differentiating invasive from non-invasive breast cancer. **b** Distribution graph of regression coefficients for the optimal radiomic features

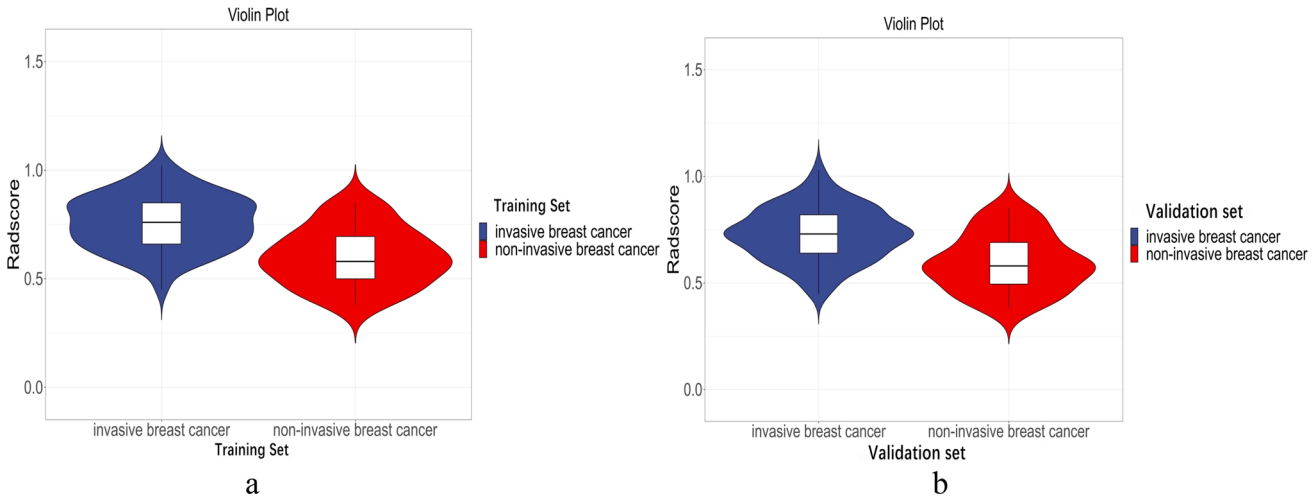

Fig. 4 Distribution of radiomics score. **a** Training set; **b** Validation set

3.3 Construction of machine learning models

Coronal plane characteristics, SWV, and Radscore were incorporated into both univariate and multivariate logistic regression analyses to identify independent factors discriminating between invasive and non-invasive breast cancer. The results showed that coronal plane features, SWV, and Radscore were each independent factors ($P < 0.05$) (Table 2). Diagnostic models were then developed based on these factors using four machine learning algorithms: LR, RF, DT, and SVM (Table 3, Fig. 5). Based on the validation set results, the DT model exhibited the highest performance, indicating its superior generalization capability. Consequently, we selected the DT model as the output model for this study and visualized the feature importance within the DT model using Shapley Additive Explanations (SHAP) values (Fig. 6).

3.4 Comparison of models

Using the DT algorithm as the output model, we first constructed imaging model based on coronal plane features and SWV, along with a radiomics label model based on Radscore. A combined model was then developed by integrating

Table 2 Presents the univariate and multivariate logistic regression analyses for discriminating between invasive and non-invasive breast cancer

Potential risk factors	Univariate analysis OR (95%CI)	*P* value	Multivariate analysis OR (95%CI)	*P* value
Coronal plane features		0.008		0.026
Coronal plane features (1)	0.944 (0.365, 2.441)		0.948 (0.278, 3.233)	
Coronal plane features (2)	5.037 (1.660, 15.287)		5.313 (1.392, 20.275)	
SWV (m/s)	4.148 (1.730, 9.944)	0.001	3.968 (1.272, 12.380)	0.018
Radscore	1.102 (1.058, 1.147)	< 0.001	1.104 (1.056, 1.155)	< 0.001

Table 3 Performance evaluation of diagnostic models constructed by four machine learning algorithms

	AUC (95%CI)	Sensitivity (%)	Specificity (%)
Model/Training set			
LR	0.880 (0.817–0.944)	72.9	91.2
RF	0.808 (0.720–0.896)	75.3	79.4
DT	0.878 (0.819–0.939)	77.6	85.3
SVM	0.860 (0.790–0.931)	74.1	88.2
Validation set			
LR	0.808 (0.633–0.982)	97.4	61.5
RF	0.787 (0.577–0.997)	94.9	76.9
DT	0.874 (0.774–0.974)	92.3	69.2
SVM	0.625 (0.453–0.797))	48.7	76.9

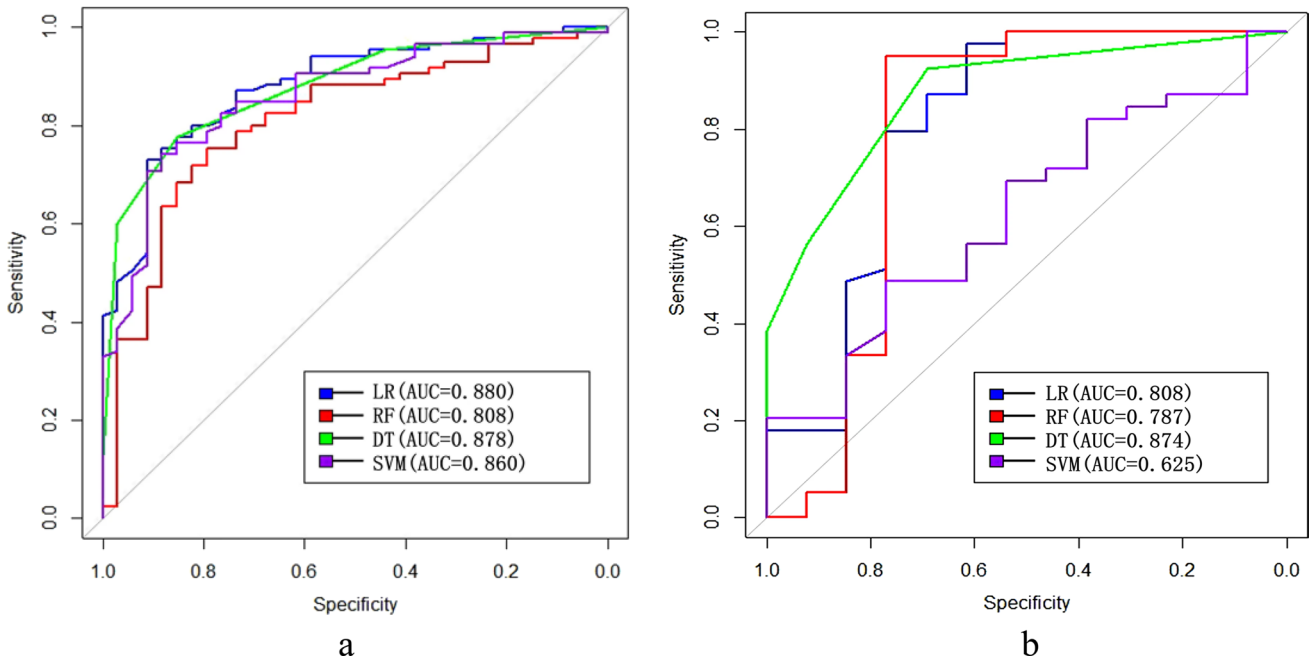

Fig. 5 ROC curves of each univariate and combined model. **a** Training set; **b** Validation set

the imaging model with the radiomics label model. The performance of the imaging model, radiomics label model, and combined model was compared using the DeLong test. In the training set, the differences between the imaging model, radiomics label model, and combined model were all statistically significant ($P < 0.05$). However, in the validation set, the differences between these models were not statistically significant ($P > 0.05$). (see Table 4, Fig. 7).

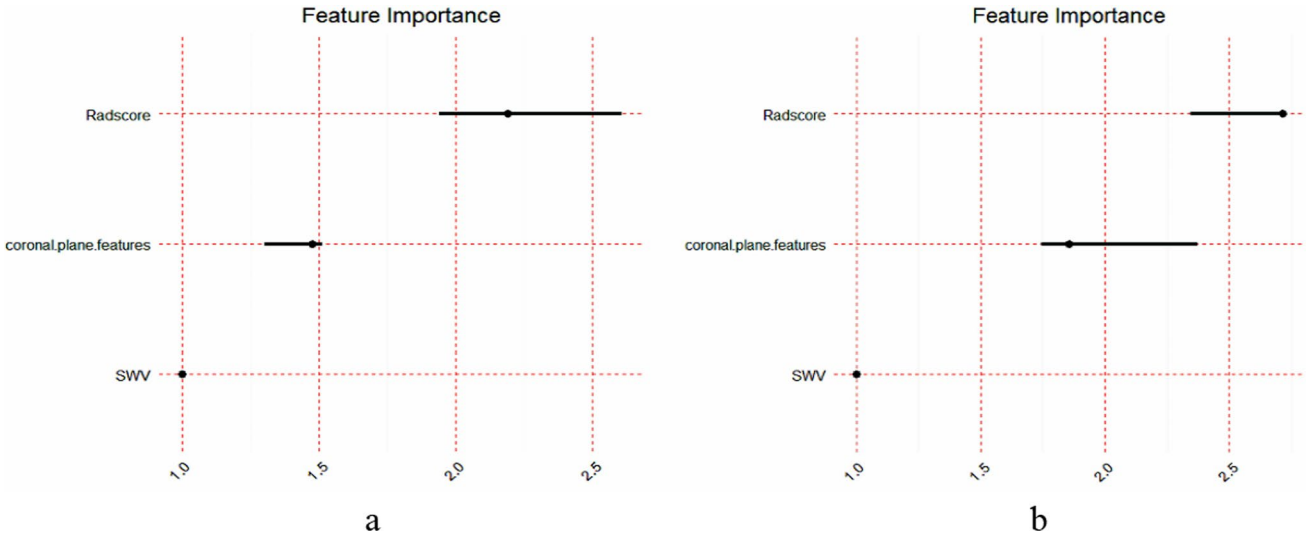

Fig. 6 presents the feature importance analysis based on SHAP values for the DT model. Panel **a** Represents the Training Set, and Panel **b** Represents the Validation Set. The figure clearly indicates that Radscore is the most influential feature in this study's DT model, significantly driving the model's decision-making process. Other features, such as coronal plane features and SWV, also contribute to the model's predictions, but their impact is less pronounced compared to Radscore

Table 4 Comparison of the Performance of Imaging Model, Radiomics Label Model, and Combined Model (DeLong Test)

	AUC (95%CI)	Sensitivity (%)	Specificity (%)	Z-Value	*P*-Value
Training set					
Imaging Model	0.734 (0.641–0.828)	48.2	85.3	−2.834	0.005
Radiomics Label Model	0.826 (0.751–0.902)	85.9	61.8	−1.977	0.048
Combined Model	0.878 (0.819–0.939)	77.6	85.3	–	–
Validation set					
Imaging Model	0.784 (0.639–0.929)	76.9	76.9	−1.246	0.213
Radiomics Label Model	0.830 (0.719–0.942)	74.4	76.9	−0.694	0.488
Combined Model	0.874 (0.774–0.974)	92.3	69.2	–	–

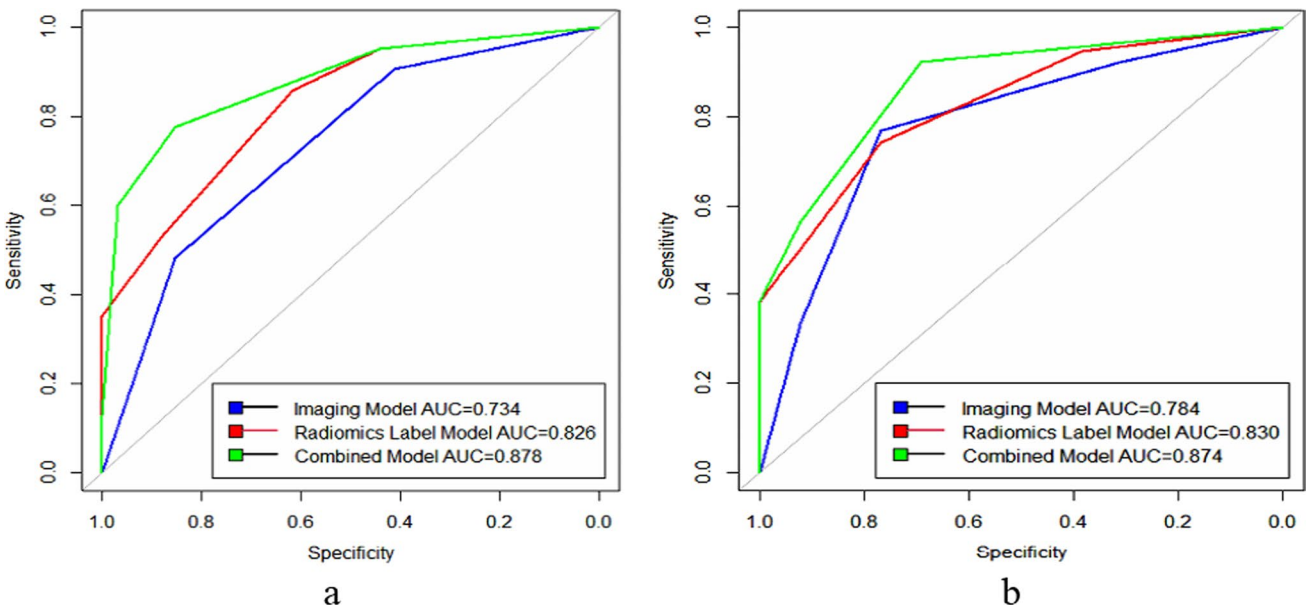

Fig. 7 ROC Curves of the Imaging Model, Radiomics Label Model, and Combined Model with the DT Algorithm as the Output Model. Panel a Represents the Training Set, and Panel b Represents the Validation Set

4 Discussion

Accurate preoperative differentiation between invasive and non-invasive breast cancer is paramount in guiding clinical treatment strategies and predicting patient outcomes. There's a notable trend of overdiagnosis of non-invasive breast cancer in clinical settings, often leading to unnecessary treatments. Historically, the preoperative distinction between these cancer types has primarily depended on biopsy procedures [13–15]. However, biopsies are invasive and may not capture the tumor's comprehensive tissue profile. With the advent and continual evolution of artificial intelligence, radiomics has emerged as a powerful tool in differentiating benign from malignant tumors, and in evaluating the risks of metastasis and recurrence [16–18]. Previous radiomic studies in breast-related pathologies have predominantly focused on MRI, leaving a gap in the exploration of ultrasound radiomics. Our study bridges this gap by leveraging high-definition coronal images from ABVS. We successfully extracted 298 radiomics features, from which 12 optimal features were identified through dimensionality reduction using the LASSO regression technique. This approach represents a significant advancement in the non-invasive assessment of breast cancer, offering a more nuanced understanding of tumor characteristics.

ABVS, with its standardized scanning protocol, offers superior repeatability, consistency, and a more comprehensive capture of lesion characteristics when compared to conventional two-dimensional ultrasound [19–21]. It records the entire breast, yielding a detailed three-dimensional coronal view, a perspective not attainable with traditional ultrasound techniques. This enhanced view facilitates the examination of breast lesions from multiple angles, enriching the diagnostic information available. A notable aspect of the ABVS coronal view is the 'convergence sign', a unique feature that has emerged as a critical marker for malignant breast nodules. Despite its significance, there has been a lack of research on employing the 'convergence sign' specifically for differentiating between invasive and non-invasive breast cancer. In our study, coronal plane features effectively capture the relationship between the tumor and surrounding tissues, which is crucial for distinguishing invasive tumors. Invasive breast cancer typically exhibits pathological characteristics such as poorly defined boundaries with surrounding tissues, irregular morphology, and infiltration into adjacent fatty tissue—features that are often more prominently displayed in coronal plane images. This may be attributed to the "convergence sign," which directly reflects the interaction between the lesion and the surrounding tissue. Invasive breast cancer grows invasively into the surrounding tissues, exerting traction on these tissues, leading to breast tissue hyperplasia and the formation of peripheral radial hyperechoic lines, thus creating the visually discernible "convergence sign." ARFI elastography, a technique that applies acoustic pulses to induce localized displacement in tissues, forms the basis of VTQ, one of the ARFI methods. VTQ operates on the principle of using sound waves to measure average SWV in a given area, offering an objective evaluation of tissue elasticity [22]. The SWV measurements in elastography correlate with tissue hardness, which in turn is indicative of the degree of fibrosis within a tumor; typically, malignant lesions, being harder than benign ones, exhibit higher SWV values. This increase in hardness, often seen in more malignant lesions, is attributed to more intricate cellular structures, increased extracellular matrix, and heightened fibrosis. Given that invasive breast cancer typically presents a higher degree of malignancy compared to its non-invasive counterpart, it tends to have a denser texture, potentially due to these factors [23].

Machine learning, a rapidly evolving branch of AI, is increasingly crucial in medical data analysis [24, 25]. In our study, the four machine learning models demonstrated significant performance differences across various datasets. These differences may be closely linked to how each algorithm processes data features, the interactions between those features, and variations in sample size. Specifically, the DT model excelled in the validation set, highlighting its strong generalization capability when managing complex feature interactions. In contrast, the LR model performed best in the training set, likely because it effectively captures linear feature relationships. However, its robustness in the validation set was compromised, potentially due to overfitting. These performance discrepancies underscore the importance of selecting the appropriate machine learning model in clinical practice. Model selection should not only consider training set performance but also prioritize generalization ability on independent validation sets to ensure reliability in real-world applications. Our findings suggest that integrating radiomics with machine learning techniques holds substantial potential for preoperative differentiation between breast cancer types.

Our study presents several limitations that warrant consideration. Firstly, it is a retrospective analysis, inherently susceptible to potential selection biases. Secondly, the sample size of our research cohort is comparatively limited, which may impact the generalizability of our findings. Lastly, our results have not undergone external validation. To address these limitations and reinforce the validity of our findings, we are planning future multicenter research initiatives aimed at further substantiating our results.

5 Conclusion

In conclusion, the distinction between invasive and non-invasive breast cancer through precise preoperative assessment is vital in formulating suitable treatment strategies and forecasting patient outcomes. The machine learning framework developed by integrating ABVS radiomics with VTQ has shown efficacy in the preoperative differentiation of these cancer types. While the performance in the RF and SVM evaluations within the test dataset exhibited a lower effectiveness (AUC < 0.80), the other models within this framework have demonstrated reliable accuracy in this differentiation task. Notably, the use of SHAP values enhances interpretability, aiding clinicians in crafting individualized treatment plans based on specific diagnostic insights.

Acknowledgements Thank you to all the friends who provided help and support during the data collection process of the thesis.

Author contributions LF, YW, SW, CZ, XZ contributed to the study conception and design. The frst draft of the manuscript was written by LF and all authors commented on previous versions of the manuscript. LF, YW, SW, CZ, XZ read and approved the final manuscript.

Funding Major Project for the Construction of Peak Disciplines in Universities by the Education Department of Anhui Province (GXXK-2020-44). Key Scientific Research Project in Natural Sciences for Universities by the Education Department of Anhui Province (2023AH051743). The open project of Anhui Province Key Laboratory of Cancer Translational Medicine, Bengbu Medical University (No. KFKT202307).

Data availability The datasets generated during and/or analysed during the current study are available from the first author (18895348832@163.com) on reasonable request.

Code availability Not applicable.

Declarations

Ethics approval and consent to participate This investigation was conducted in strict accordance with the ethical guidelines set forth in the Declaration of Helsinki, and was reviewed and approved by the Ethics Committee of Wannan Medical College (IRB No. 102, 2023). As this study is a retrospective analysis, the requirement for informed consent was waived by the Ethics Committee.

Competing interests The authors have no relevant financial or non-financial interests to disclose.

References

1. Chen W, Ru R, Wang F, et al. Automated breast volume scanning combined with shear wave elastography for diagnosis of triple-negative breast cancer and human epidermal growth factor receptor 2-positive breast cancer. Rev Assoc Med Bras (1992). 2021;67(8):1167–71.
2. Ouyang F, Guo B, Huang X, et al. A nomogram for individual prediction of vascular invasion in primary breast cancer. Eur J Radiol. 2019;110:30–8.
3. Galati G, De Vincentis A, Gallo P, et al. Diagnostic value of Virtual Touch Quantification (VTQ®) for differentiation of hemangiomas from malignant focal liver lesions. Med Ultrason. 2019;21(4):371–6.
4. Jakub J, Murphy B, Gonzalez A, et al. A validated nomogram to predict upstaging of ductal carcinoma in situ to invasive disease. Ann Surg Oncol. 2017;24(10):2915–24.
5. Maeda H, Hayashida T, Watanuki R, et al. Predictors of invasive disease in patients preoperatively diagnosed with ductal carcinoma without stromal invasion, with breast magnetic resonance imaging (MRI) and ultrasound (US). Breast Cancer. 2021;28(2):398–404.
6. Ohira R, Yanagawa M, Suzuki Y, et al. CT-based radiomics analysis for differentiation between thymoma and thymic carcinoma. J Thorac Dis. 2022;14(5):1342–52.
7. Lin X, Zhao S, Jiang H, et al. A radiomics-based nomogram for preoperative T staging prediction of rectal cancer. Abdom Radiol (NY). 2021;46(10):4525–35.
8. Bian T, Wu Z, Lin Q, et al. Evaluating tumor-infiltrating lymphocytes in breast cancer using preoperative MRI-based radiomics. J Magn Reson Imaging. 2022;55(3):772–84.
9. Wang S, Liu H, Yang T, et al. Automated breast volume scanner (ABVS)-based radiomic nomogram: a potential tool for reducing unnecessary biopsies of BI-RADS 4 lesions. Diagnostics (Basel). 2022;12(1):172.

10. Wan J, Wu R, Yao M, et al. Acoustic radiation force impulse elastography in evaluation of triple-negative breast cancer: a preliminary experience. Clin Hemorheol Microcirc. 2018;70(3):301–10.
11. Zengel P, Notter F, Clevert DA. VTIQ and VTQ in combination with B-mode and color Doppler ultrasound improve classification of salivary gland tumors, especially for inexperienced physicians. Clin Hemorheol Microcirc. 2018;70(4):457–66.
12. Yang YP, Xu XH, Bo XW, et al. Comparison of virtual touch tissue imaging & quantification (VTIQ) and virtual touch tissue quantification (VTQ) for diagnosis of thyroid nodules. Clin Hemorheol Microcirc. 2017;65(2):137–49.
13. Yampaka T, Noolek D. Data driven for early breast cancer staging using integrated mammography and biopsy. Asian Pac J Cancer Prev. 2021;22(12):4069–74.
14. Shanmugalingam A, Hitos K, Hegde S, et al. Concordance between core needle biopsy and surgical excision for breast cancer tumor grade and biomarkers. Breast Cancer Res Treat. 2022;193(1):151–9.
15. Slostad JA, Yun NK, Schad AE, et al. Concordance of breast cancer biomarker testing in core needle biopsy and surgical specimens: a single institution experience. Cancer Med. 2022;11(24):4954–65.
16. Sammour T, Bedrikovetski S. Radiomics for diagnosing lateral pelvic lymph nodes in rectal cancer: Artificial intelligence enabling precision medicine? Ann Surg Oncol. 2020;27(11):4082–3.
17. Calabrese A, Santucci D, Landi R, et al. Radiomics MRI for lymph node status prediction in breast cancer patients: the state of art. J Cancer Res Clin Oncol. 2021;147(6):1587–97.
18. Jiang Y, Zhang Z, Yuan Q, et al. Predicting peritoneal recurrence and disease-free survival from CT images in gastric cancer with multitask deep learning: a retrospective study. Lancet Digit Health. 2022;4(5):e340–50.
19. Wang X, Tao L, Zhou X, et al. Initial experience of automated breast volume scanning (ABVS) and ultrasound elastography in predicting breast cancer subtypes and staging. Breast. 2016;30:130–5.
20. Girometti R, Zanotel M, Londero V, et al. Automated breast volume scanner (ABVS) in assessing breast cancer size: a comparison with conventional ultrasound and magnetic resonance imaging. Eur Radiol. 2018;28(3):1000–8.
21. Liu J, Zhou Y, Wu J, et al. Diagnostic performance of combined use of automated breast volume scanning & hand-held ultrasound for breast lesions. Indian J Med Res. 2021;154(2):347–54.
22. Pu H, Zhao LX, Yao MH, et al. Conventional US combined with acoustic radiation force impulse (ARFI) elastography for prediction of triple-negative breast cancer and the risk of lymphatic metastasis. Clin Hemorheol Microcirc. 2017;65(4):335–47.
23. Magalhães M, Belo-oliveira P, Casalta-lopes J, et al. Diagnostic value of ARFI (Acoustic Radiation Force Impulse) in differentiating benign from malignant breast lesions. Acad Radiol. 2017;24(1):45–52.
24. Liu G, Poon M, Zapala M, et al. Incorporating radiomics into machine learning models to predict outcomes of neuroblastoma. J Digit Imaging. 2022;35(3):605–12.
25. Nakanishi R, Slomka P, Riso R, et al. Machine learning adds to clinical and CAC assessments in predicting 10-Year CHD and CVD Deaths. JACC Cardiovasc Imaging. 2021;14(3):615–25.